nature neuroscience

Neuregulin 1 regulates excitability of fast-spiking neurons through Kv1.1 and acts in epilepsy

Ke-Xin Li[1], Ying-Mei Lu[1], Zheng-Hao Xu[1], Jing Zhang[1], Jun-Ming Zhu[2], Jian-Ming Zhang[2], Shu-Xia Cao[1], Xiao-Juan Chen[1], Zhong Chen[1], Jian-Hong Luo[1,3], Shumin Duan[1,3] & Xiao-Ming Li[1,3]

Dysfunction of fast-spiking, parvalbumin-positive (FS-PV) interneurons is implicated in the pathogenesis of epilepsy. ErbB4, a key Neuregulin 1 (NRG1) receptor, is mainly expressed in this type of interneurons, and recent studies suggest that parvalbumin interneurons are a major target of NRG1-ErbB4 signaling in adult brain. Thus, we hypothesized that downregulation of NRG1-ErbB4 signaling in FS-PV interneurons is involved in epilepsy. We found that NRG1, through its receptor ErbB4, increased the intrinsic excitability of FS-PV interneurons. This effect was mediated by increasing the near-threshold responsiveness and decreasing the voltage threshold for action potentials through Kv1.1, a voltage-gated potassium channel. Furthermore, mice with specific deletion of ErbB4 in parvalbumin interneurons were more susceptible to pentylenetetrazole- and pilocarpine-induced models of epilepsy. Exogenous NRG1 delayed the onset of seizures and decreased their incidence and stage. Moreover, expression of ErbB4, but not ErbB2, was downregulated in human epileptogenic tissue. Together, our findings suggest that NRG1–ErbB4 signaling contributes to human epilepsy through regulating the excitability of FS-PV interneurons. ErbB4 may be a new target for anticonvulsant drugs in epilepsy.

Epilepsy is a disabling neurological disorder that affects about 1% of the general population of all ages. About 30% of affected individuals continue to have breakthrough seizures despite appropriate pharmacological anticonvulsant treatment[1], and surgical removal of the epileptic focus is suitable only for a minority. Understanding the causes of the pathology underlying the occurrence of seizures is necessary and urgent for finding effective and safe treatments.

Fast-spiking interneurons expressing the calcium-binding protein parvalbumin, comprising 40–50% of GABAergic interneurons, are the dominant inhibitory system in neocortex. They preferentially project their axons onto the perisomatic region of target neurons, regulating the output of pyramidal neurons[2]. Dysfunction of the fast-spiking interneurons is implicated in the pathogenesis of epilepsy[3,4]. Thus, the causal link between reduced fast-spiking interneuron–mediated inhibition and seizures has directed our efforts to counteract the loss of inhibition by increasing their activity.

NRG1 is a member of a family of neurotrophic factors that acts by activating the tyrosine kinase of ErbB receptors, including ErbB4 (refs. 5–7). In adult brains, *Erbb4* mRNA is enriched in regions where interneurons are clustered[8]. Furthermore, ErbB4 expression is largely confined to specific classes of interneurons, particularly parvalbumin cells[9–13]. NRG1 regulates GABAergic transmission[13]. In addition, recent studies demonstrate that ErbB4 in parvalbumin interneurons is critical for NRG1 regulation of pyramidal neuronal activity and long-term potentiation (LTP) in adult brain[14–17]. All these studies suggest that parvalbumin interneurons are a major cellular target of NRG1-ErbB4 signaling in adult brain, and the causal link between reduced FS-PV interneuron–mediated inhibition and seizures led us to hypothesize that dysfunction of NRG1-ErbB4 is involved in epilepsy.

Here we investigated whether NRG1-ErbB4 directly regulates the excitability of FS-PV interneurons and the underlying mechanisms. Furthermore, we determined whether there is a link between downregulated NRG1-ErbB4 signaling and epilepsy in adult brain. We found that NRG1, through its receptor ErbB4, increased the excitability of FS-PV interneurons. This effect was mediated by decreasing the voltage threshold through Kv1.1. Furthermore, mice with specific deletion of ErbB4 in parvalbumin interneurons were more susceptible to animal models of epilepsy. Expression of ErbB4 was also reduced in human epileptogenic tissue. Our findings suggest that ErbB4 may be a target for the development of a new class of anticonvulsant drugs.

RESULTS

NRG1 increases the excitability of FS-PV interneurons

To investigate whether NRG1-ErbB4 signaling regulates the function of FS-PV interneurons, we first performed whole-cell current-clamp recordings in acute cortical slices from the transgenic mouse lines B13 and G42 expressing enhanced green fluorescent protein (EGFP) in most parvalbumin interneurons. Expression in these lines is well characterized[2,18–20] as effectively targeting fast-spiking cells. Further identification of fast-spiking cells by measuring their membrane properties and firing patterns was based upon their distinctive

[1]Department of Neurobiology, Key Laboratory of Medical Neurobiology of Ministry of Health of China, Zhejiang Province Key Laboratory of Neurobiology, Zhejiang University School of Medicine, Hangzhou, Zhejiang, China. [2]Department of Neurosurgery, Second Affiliated Hospital, Zhejiang University School of Medicine, Hangzhou, Zhejiang, China. [3]Soft Matter Research Center, Zhejiang University, Hangzhou, Zhejiang, China. Correspondence should be addressed to X.-M.L. (lixm@zju.edu.cn).

Received 13 May; accepted 7 November; published online 11 December 2011; doi:10.1038/nn.3006

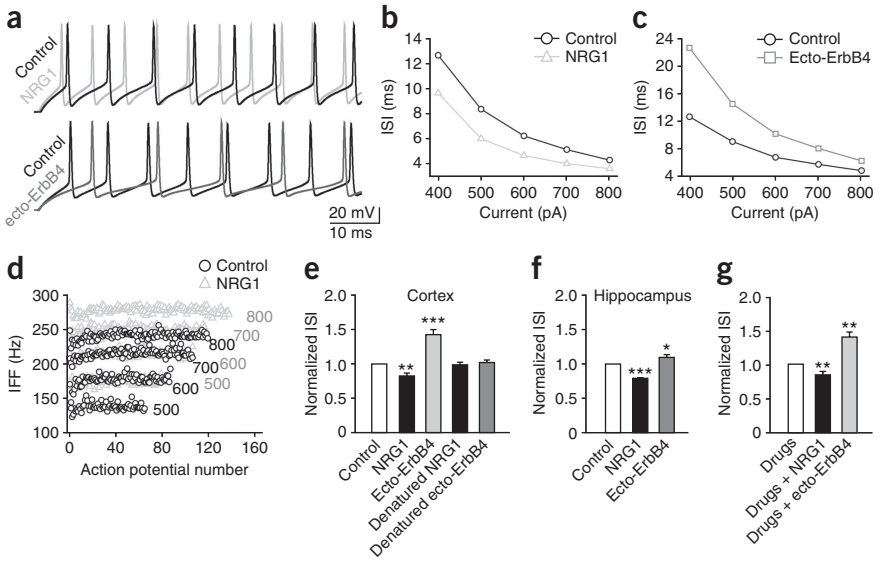

Figure 1 Both exogenous and endogenous NRG1 increase the excitability of cortical and hippocampal FS-PV interneurons. (**a**) Representative action potentials of two FS-PV interneurons in cortical layers 2/3 before (black) and after bath application of 10 nM NRG1 (top, light gray) or 2 μg ml^{-1} ecto-ErbB4 (bottom, dark gray). (**b**,**c**) Plots of ISI before and after bath application of NRG1 (**b**) or ecto-ErbB4 (**c**). (**d**) Plot of instantaneous firing frequency (IFF, quantified as the inverse of the ISI), illustrating spike frequency acceleration after bath application of NRG1. (**e**) Normalized ISI of cortical layer 2/3 FS-PV interneurons before and after bath application of 10 nM NRG1, 2 μg ml^{-1} ecto-ErbB4, 10 nM denatured NRG1 or 2 μg ml^{-1} denatured ecto-ErbB4. $n = 7$ or 8; $^{**}P < 0.01$, $^{***}P < 0.001$. (**f**) Normalized ISI of hippocampal FS-PV interneurons before and after bath application of 10 nM NRG1 or 2 μg ml^{-1} ecto-ErbB4. $n = 6$ or 7; $^{*}P < 0.05$, $^{***}P < 0.001$. (**g**) Normalized ISI in the presence of drugs (50 μM DL-AP5, 20 μM DNQX and 100 μM picrotoxin) before (drugs) and after 10 nM NRG1 (drugs + NRG1) or 2 μg ml^{-1} ecto-ErbB4 (drugs + ecto-ErbB4). $n = 7$; $^{**}P < 0.01$. Error bars represent s.e.m.

characteristics[18] (**Supplementary Table 1**). Neuronal excitability was measured by a series of 500-ms-step current injections. Patch clamp recordings showed that bath application of 10 nM NRG1 decreased the average interspike interval (ISI) (82.9 ± 3.1% of the control; $P < 0.01$; **Fig. 1**) and increased the firing frequency (**Fig. 1d** and **Supplementary Fig. 1a**). It has been reported that NRG1 is endogenously expressed and released by neurons and glia[13,21]. To determine whether endogenous NRG1 regulates the excitability of fast-spiking interneurons, we then interfered with the activity of endogenous NRG1 by applying ecto-ErbB4, a NRG1-neutralizing peptide. Ecto-ErbB4 (2 μg ml^{-1}) substantially dampened the excitability of fast-spiking interneurons by prolonging ISI (142.8 ± 7.2% of the control; $P < 0.001$; **Fig. 1a**,**c**,**e**) or by decreasing the firing frequency (**Supplementary Fig. 1b**). This effect seemed specific because it was abolished by heat inactivation of NRG1 or ecto-ErbB4 (**Fig. 1e**).

To examine whether NRG1 also regulates the excitability of fast-spiking interneurons in other brain regions, we performed the same recordings on FS-PV cells in mouse hippocampus. ISI decreased after NRG1 treatment but increased after ecto-ErbB4 treatment (**Fig. 1f**), consistent with results in neocortical FS-PV interneurons.

Some studies have shown that NRG1 regulates synaptic currents[9,13,22–25], so the effect of NRG1 on fast-spiking cell excitability could be caused by (i) the excitatory or inhibitory input onto fast-spiking cells or (ii) direct modulation of the intrinsic excitability of fast-spiking cells. To discriminate between these two possibilities, we blocked synaptic inputs with the NMDA receptor antagonist DL-2-amino-5-phosphonovaleric acid (DL-AP5; 50 μM), AMPA and kainate receptor antagonist 6,7-dinitroquinoxaline-2,3-dione (DNQX; 20 μM) and $GABA_A$ receptor antagonist picrotoxin (100 μM) and found that the effect of NRG1 or ecto-ErbB4 on ISI remained (**Fig. 1g**), suggesting that NRG1 directly affects the intrinsic properties of FS-PV interneurons.

To determine whether NRG1 specifically acts on fast-spiking cells, we recorded from layer 2/3 pyramidal neurons. Pyramidal neurons were indentified by their prominent apical dendrites and adaptive firing (**Supplementary Table 1**). Treatment with NRG1 decreased the excitability of layer 2/3 pyramidal neurons. Within 500 ms of current injection, there was a reduction of action potential numbers from 14.83 ± 1.42 to 11.83 ± 1.30 after treatment with NRG1 (**Supplementary Fig. 2a**,**b**). This is in agreement with a previous study[14]. However, this effect was abolished by picrotoxin (100 μM), a $GABA_A$ receptor antagonist (**Supplementary Fig. 2c**), suggesting that the effect of NRG1 on pyramidal neurons is mediated by GABAergic transmission. To determine whether NRG1 regulates the GABAergic transmission onto pyramidal neurons, inhibitory postsynaptic currents (IPSCs) were recorded from layer 2/3 pyramidal neurons. Bath application of NRG1 increased both the amplitude and frequency of spontaneous IPSCs (**Supplementary Fig. 2d**,**e**). In contrast, it had no effect on miniature IPSCs (mIPSCs) (**Supplementary Fig. 2f**). These results indicate that NRG1 indirectly regulates the excitability of pyramidal neurons through activity-dependent GABAergic transmission. Taken together, our findings indicated that NRG1 directly regulates the intrinsic excitability of FS-PV interneurons.

ErbB4 mediates NRG1's effect on FS-PV excitability

ErbB4 is highly expressed in parvalbumin interneurons of adult brain[8,9]. To determine whether NRG1 regulates the excitability of FS-PV interneurons through ErbB4 receptors, we first used a pharmacological approach by treatment with the ErbB4 antagonist AG1478, which specifically prevents ErbB4 signaling[26]. Treatment with AG1478 prevented the NRG1-induced decrease in the ISI (**Fig. 2a**). This result suggests a role of ErbB4 in the regulation of fast-spiking interneuron excitability by NRG1. AG1478 alone substantially suppressed the excitability of fast-spiking interneurons by prolonging ISI (137 ± 12.7% of control, $P < 0.01$; **Fig. 2a**), providing further evidence that endogenous NRG1 activity may be necessary to maintain the intrinsic excitability of fast-spiking cells.

Then, to confirm this effect, we used the Cre-*loxP* genetic approach to ablate ErbB4 expression specifically in parvalbumin interneurons by crossing *Erbb4*$^{loxP/loxP}$ mice[27] with *Pvalb-cre* mice[27–29] (**Fig. 2b**). To determine the extent of ErbB4 deletion in parvalbumin interneurons, we stained cortical sections with antibodies to parvalbumin and ErbB4. In control littermates, ErbB4 was detectable in almost all parvalbumin interneurons and in neurons that were not positive for parvalbumin (**Fig. 2c**), in agreement with previous studies[9,11,12,30,31]. In *Pvalb-cre;Erbb4*$^{-/-}$ sections, by contrast, ErbB4 immunoreactivity was abolished in parvalbumin interneurons, but not in parvalbumin-negative

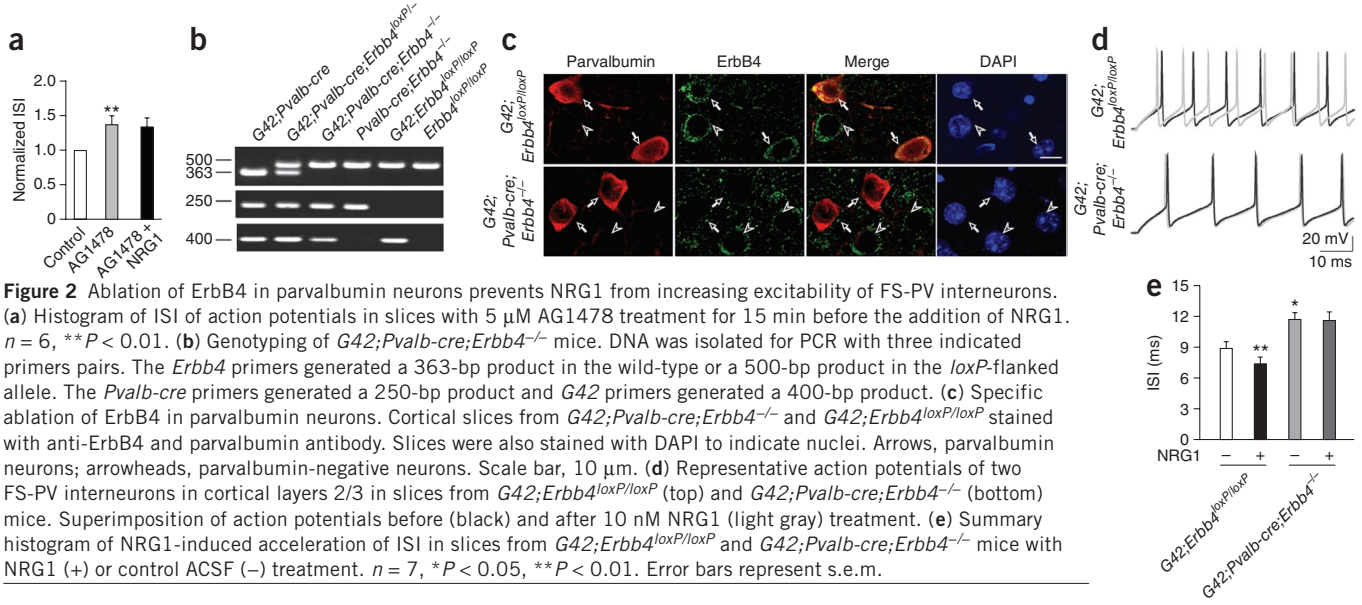

Figure 2 Ablation of ErbB4 in parvalbumin neurons prevents NRG1 from increasing excitability of FS-PV interneurons. (**a**) Histogram of ISI of action potentials in slices with 5 μM AG1478 treatment for 15 min before the addition of NRG1. $n = 6$, $^{**}P < 0.01$. (**b**) Genotyping of *G42;Pvalb-cre;Erbb4*$^{-/-}$ mice. DNA was isolated for PCR with three indicated primers pairs. The *Erbb4* primers generated a 363-bp product in the wild-type or a 500-bp product in the *loxP*-flanked allele. The *Pvalb-cre* primers generated a 250-bp product and *G42* primers generated a 400-bp product. (**c**) Specific ablation of ErbB4 in parvalbumin neurons. Cortical slices from *G42;Pvalb-cre;Erbb4*$^{-/-}$ and *G42;Erbb4*$^{loxP/loxP}$ stained with anti-ErbB4 and parvalbumin antibody. Slices were also stained with DAPI to indicate nuclei. Arrows, parvalbumin neurons; arrowheads, parvalbumin-negative neurons. Scale bar, 10 μm. (**d**) Representative action potentials of two FS-PV interneurons in cortical layers 2/3 in slices from *G42;Erbb4*$^{loxP/loxP}$ (top) and *G42;Pvalb-cre;Erbb4*$^{-/-}$ (bottom) mice. Superimposition of action potentials before (black) and after 10 nM NRG1 (light gray) treatment. (**e**) Summary histogram of NRG1-induced acceleration of ISI in slices from *G42;Erbb4*$^{loxP/loxP}$ and *G42;Pvalb-cre;Erbb4*$^{-/-}$ mice with NRG1 (+) or control ACSF (–) treatment. $n = 7$, $^{*}P < 0.05$, $^{**}P < 0.01$. Error bars represent s.e.m.

neurons (**Fig. 2c**). These results demonstrated the specific loss of ErbB4 in parvalbumin interneurons. To assist electrophysiological recording from FS-PV interneurons, *Pvalb-cre;Erbb4*$^{-/-}$ mice were further crossed with *G42;Erbb4*$^{loxP/loxP}$ mice, where *G42* represents *Gad1-EGFP* line G42, in which the parvalbumin-positive subset of GABAergic neurons are fluorescently labeled. Then we tested the effect of NRG1 in slices from parvalbumin-specific ErbB4 knockout mice. In contrast to the abbreviation of ISI by NRG1 treatment in *G42;Erbb4*$^{loxP/loxP}$ mice (8.9 ± 0.7 ms to 7.4 ± 0.6 ms, $P < 0.01$; **Fig. 2d**,**e**), there was no change in ISI by NRG1 applied in *G42;Pvalb-cre;Erbb4*$^{-/-}$ mice. *G42;Pvalb-cre;Erbb4*$^{-/-}$ mice also had a reduced intrinsic excitability of fast-spiking interneurons, as shown by a prolonged ISI (8.9 ± 0.5 ms to 11.7 ± 0.7 ms; $P < 0.05$; **Fig. 2d**,**e**), consistent with pharmacological inhibition of ErbB4 (**Fig. 2a**) and in further support of the involvement of endogenous NRG1 in regulating the excitability of fast-spiking interneurons. These results indicate that ErbB4 is critical for the regulation of FS-PV interneuronal excitability by NRG1.

NRG1 decreases the voltage threshold of action potentials

To investigate the mechanisms underlying the NRG1 regulation of FS-PV interneuron excitability, we further analyzed the action potential parameters. NRG1 increased the slope of initiation, whereas ecto-ErbB had the opposite effect (**Fig. 3a**). Plots of membrane potential rate of change dV/dt versus membrane potential showed that the voltage threshold for action potential generation shifted to more hyperpolarized levels (−40.2 ± 1.47 mV to −43.6 ± 1.26 mV, $P < 0.01$; **Fig. 3b**,**c**) after NRG1 treatment, whereas they shifted to more depolarized levels (−40.9 ± 1.09 mV to −35.8 ± 1.54 mV, $P < 0.01$; **Fig. 3c**) after ecto-ErbB4 treatment. However, we found no significant change in other spike shape parameters, including afterhyperpolarization (−21.8 ± 1.65 mV to −22.1 ± 1.92 mV; $P = 0.45$), amplitude (68.5 ± 0.94 mV to 67.6 ± 1.64 mV; $P = 0.44$) and half-width (0.34 ± 0.01 ms to 0.35 ± 0.01 ms; $P = 0.25$) after NRG1 treatment. We also checked the voltage threshold for the generation of action potentials in FS-PV interneurons in slices from *G42;Erbb4*$^{loxP/loxP}$ and *G42;Pvalb-cre;Erbb4*$^{-/-}$ mice. FS-PV interneurons in slices from *G42;Pvalb-cre;Erbb4*$^{-/-}$ mice had a more depolarized voltage threshold for action potential generation (−34.4 ± 1.1 mV) than those from *G42;Erbb4*$^{loxP/loxP}$ mice (−40.0 ± 1.1 mV, $P < 0.01$), providing *in vivo* evidence that ErbB4 is important in the regulation of action potential generation of FS-PV interneurons.

Next we measured passive membrane properties, including input resistance, resting membrane potential, membrane time constant and membrane capacitance, and found no significant difference with NRG1 treatment (**Supplementary Fig. 3a**–**d**). These results indicated that NRG1 treatment does not affect the passive membrane properties of these neurons.

To confirm the effect of NRG1 on the voltage threshold for action potential generation, we directly measured the threshold current for action potential generation by probing with small current steps[18]. With the increase of injected current, all FS-PV interneurons showed high-frequency discharges. Ecto-ErbB4 alone reversibly increased the threshold current (**Fig. 4a**,**b**) and suppressed the excitability of fast-spiking interneurons in the absence of exogenous NRG1, as shown by a decreased firing frequency ($P < 0.001$; **Fig. 4c**). The inhibitory effect was evident within 5 min of ecto-ErbB4 application, reached a maximum at 15 min and disappeared about 15 min after the removal of ecto-ErbB4. The effect of NRG1 on the threshold current was opposite to that described for the application of ecto-ErbB4 (**Supplementary Fig. 4a**,**b**). These results indicated that NRG1 influences the excitability of FS-PV cells by regulating the near-threshold responsiveness (the slope of spike initiation) and action potential threshold.

Kv1.1 is a molecular target of NRG1-ErbB4 signaling

Considering that the Kv1 subfamily of voltage-gated potassium channels operate at near-threshold potentials[18,32,33], we hypothesized that Kv1 channels are targets for the modulation of FS-PV interneuronal excitability by NRG1. To test this hypothesis, we used electrophysiological and biochemical approaches. In agreement with a previous study, our data showed that the Kv1.1-specific blocker DTx-K[34] reduced the threshold current for action potential generation (**Fig. 4d** and **Supplementary Fig. 5**) and increased the firing frequency (**Fig. 4e** and **Supplementary Fig. 5**). Moreover, treatment with DTx-K prevented ecto-ErbB4 from increasing the threshold current and decreasing the firing frequency (**Fig. 4d**,**e**), suggesting that the regulation of FS-PV interneuronal excitability by NRG1 is mediated by DTx-K-sensitive potassium channels.

To investigate the involvement of DTx-K-sensitive potassium channels further, we first carried out voltage-clamp recordings to determine whether the overall K^+ current was changed by neutralizing the activity of endogenous NRG1 with ecto-ErbB4. We applied a series of

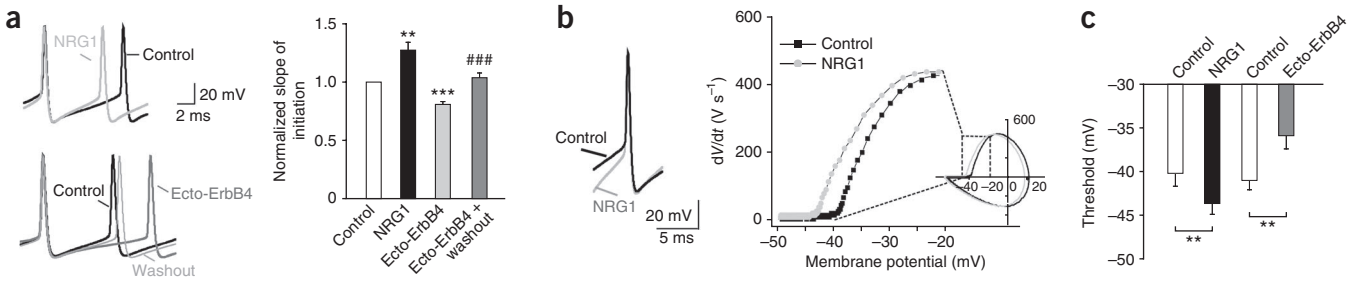

Figure 3 Enhancement of initiation of action potential in FS-PV interneurons by NRG1. (**a**) Left, superimposed action potentials from a representative FS-PV interneuron (top) before (black) and after 10 nM NRG1 (light gray) and from another FS-PV interneuron (bottom) before (black) and after 2 μg ml^{-1} ecto-ErbB4 (dark gray) application, then washout (light gray) during sustained discharge. Right, summary plot of normalized slope of initiation under indicated conditions. $n = 7$, $^{**}P < 0.01$, $^{***}P < 0.001$; $^{\#\#\#}P < 0.001$ versus ecto-ErbB4. (**b**) Left, superimposed truncated action potentials recorded before (black) and after (light gray) NRG1 application. Right, phase plane plot (V_m versus dV/dt) for action potentials before and after bath application of NRG1. Voltage threshold was defined as dV/dt = 10 mV ms^{-1}. The region around threshold has been magnified for clarity. (**c**) Summary histograms of NRG1's effects on voltage threshold. $n = 8$, $^{**}P < 0.01$. Error bars represent s.e.m.

voltage clamp pulses from −80 mV to −20 mV to generate a K^+ current with a maximal contribution from the Kv1.1 channels.

Current subtraction analysis was used to separate the DTx-K-sensitive or ecto-ErbB4-regulated current components. Subtraction of currents in the presence from those in the absence of ecto-ErbB4 (**Fig. 5a**) revealed a K^+ current component that was regulated by ecto-ErbB4 (**Fig. 5a**, bottom). Subtraction of currents in the presence from those in the absence of DTx-K (**Fig. 5b**) revealed a Kv1.1 channel current component (**Fig. 5b**, bottom) that was sensitive to DTx-K. Ecto-ErbB4 application upregulated the outward K^+ currents, which were completely inhibited by subsequent treatment with DTx-K (**Fig. 5a**,**c**). Moreover, when brain slices were pretreated with DTx-K, the K^+ currents upregulated by ecto-ErbB4 were totally abolished (**Fig. 5b**,**d**). These results indicated that the whole current regulated by ecto-ErbB4 was DTx-K sensitive. Next we compared the amplitude and voltage dependence of the DTx-K-sensitive component with (**Fig. 5a**) and without (**Fig. 5b**) ecto-ErbB4 application and found about a doubling in the amplitude after ecto-ErbB4 treatment (**Fig. 5e**). Together, the above results demonstrated that endogenous NRG1 has a powerful inhibitory effect on the Kv1.1 channel current.

There are two possible means for the regulation of Kv1.1 channels by NRG1-ErbB4: one is changing the number of channels on the membrane, and the other is regulating channel phosphorylation. First, to test the expression of Kv1.1 with or without NRG1 treatment, we performed western blots with Kv1.1α subunit-specific antibodies, which revealed no significant change in the levels of Kv1.1 after NRG1 treatment (**Fig. 5f** and **Supplementary Fig. 6**).

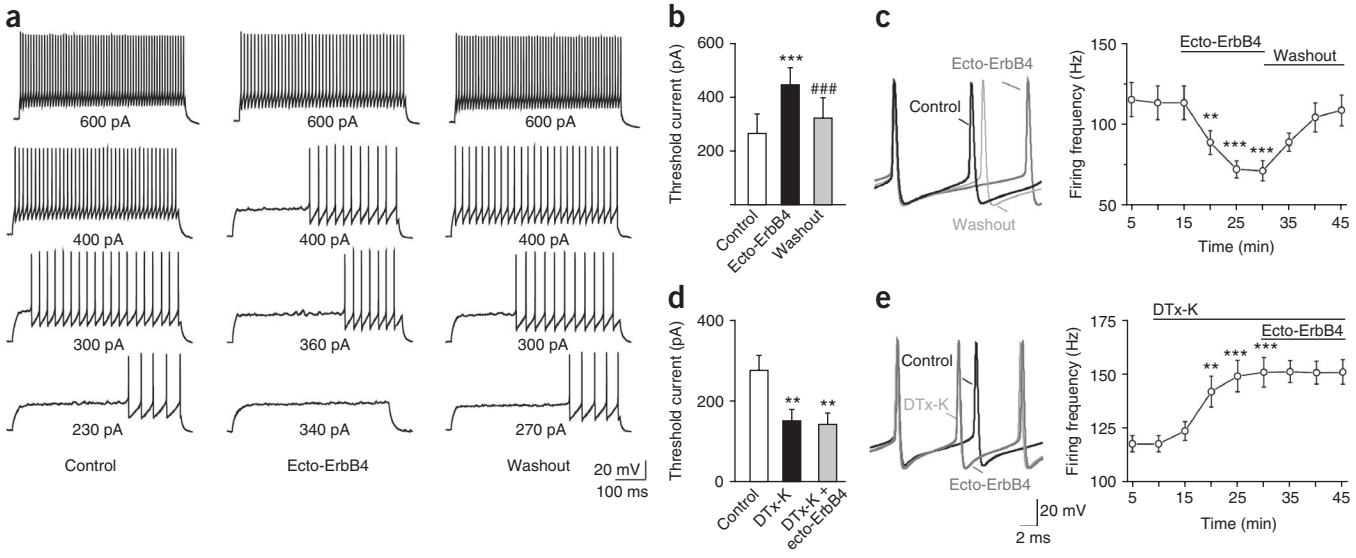

Figure 4 Reversible increase of threshold current for action potential generation by ecto-ErbB4 and inhibition by DTx-K. (**a**) Left, voltage response of a representative FS-PV interneuron in layer 2/3 of mouse cortex to current injections of, from bottom to top, 230 (the threshold current for spike generation (I_{TH})), 300, 400 and 600 pA. Middle, same interneuron as in left panel after bath application of 2 μg ml^{-1} ecto-ErbB4. Current injections, from bottom to top, 340, 360 (I_{TH}), 400 and 600 pA. Right, same interneuron as in middle after washout of ecto-ErbB4. Current injections, from bottom to top, 270 (I_{TH}), 300, 400 and 600 pA. (**b**) Summary histogram of threshold current before and after ecto-ErbB4 application and then washout. $n = 7$, $^{***}P < 0.001$; $^{\#\#\#}P < 0.001$ versus ecto-ErbB4. (**c**) Left, superimposed action potentials from a representative FS-PV interneuron before (black) and after 2 μg ml^{-1} ecto-ErbB4 (dark gray) application, then washout (light gray) during sustained discharge. Right, summary plot of firing frequency over time. $n = 8$, $^{**}P < 0.01$, $^{***}P < 0.001$. (**d**) Summary histogram of threshold current before and after DTx-K application and further treatment with ecto-ErbB4. $n = 7$, $^{**}P < 0.01$. (**e**) As in **c**, before (black) and after DTx-K (light gray) application and further ecto-ErbB4 treatment (dark gray) during sustained discharge. $n = 6$, $^{**}P < 0.01$, $^{***}P < 0.001$. Error bars represent s.e.m.

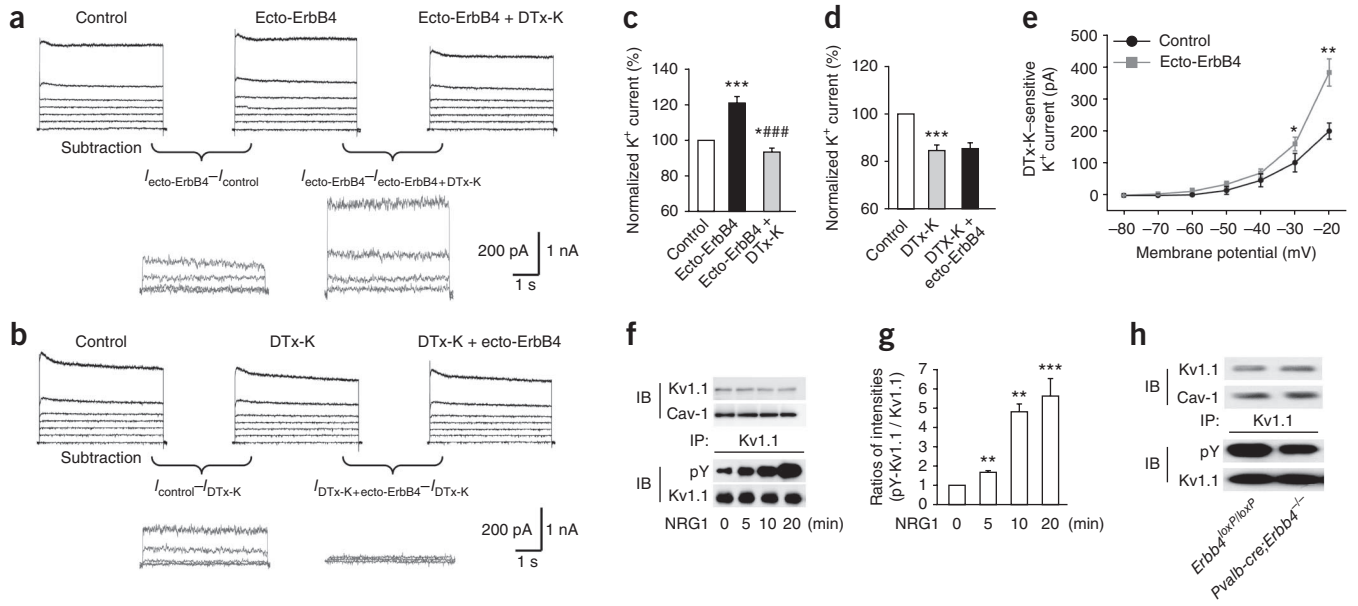

Figure 5 NRG1-ErbB4 signaling regulates Kv1.1 channels. (**a**) Top, current evoked by voltage clamping an FS-PV interneuron from –80 to –20 mV before (left) and after (middle) 2 μg ml^{-1} ecto-ErbB4 application and further addition of 100 nM DTx-K (right); bottom, current subtraction analysis. (**b**) As in **a**, top, before (left) and after (middle) 100 nM DTx-K application and further addition of 2 μg ml^{-1} ecto-ErbB4; bottom, current subtraction analysis. (**c**) Summary histogram of overall outward K^+ current activated at depolarizing voltage of –20 mV under control, ecto-ErbB4 and ecto-ErbB4 + DTx-K conditions. Results are percentage of outward K^+ current amplitude before drug administration normalized to 100%. $n = 8$, $^*P < 0.05$; $^{***}P < 0.001$; $^{\#\#\#}P < 0.001$ versus ecto-ErbB4. (**d**) Summary histogram of outward K^+ current under control, DTx-K and DTx-K + ecto-ErbB4 conditions. $n = 8$, $^{***}P < 0.001$. (**e**) Plot of the voltage dependence and peak amplitude of the DTx-K-sensitive outward currents. $n = 8$, $^*P < 0.05$, $^{**}P < 0.01$. (**f**) Immunoblot (IB) of Kv1.1 (top) and coimmunoprecipitation (IP) of Kv1.1 and phosphotyrosine (pY; bottom) in cortical membrane extracts prepared from control (0 min) and 10 nM NRG1-treated slices at indicated times. Cav-1, caveolin-1 loading control. (**g**) Summary histogram of immunoblot analysis of membrane Kv1.1 pY. $n = 4$, $^{**}P < 0.01$; $^{***}P < 0.001$. (**h**) Immunoblot of Kv1.1 (top) and co-IP of Kv1.1 and pY (middle) in cortical membrane extracts prepared from *Erbb4*$^{loxp/loxp}$ and *Pvalb-cre;Erbb4* $^{-/-}$ mice. Error bars represent s.e.m. Full-length blots are presented in **Supplementary Figure 6**.

Second, to explore whether NRG1 can phosphorylate Kv1.1, we assayed coimmunoprecipitation of Kv1.1 and phosphotyrosine or phosphoserine in membrane extracts of mouse brain. Phosphotyrosine that coimmunoprecipitated with Kv1.1 from the membranes increased progressively over time after NRG1 treatment (maximum about 500% of control; **Fig. 5f**,**g**). No significant change of immunoreaction was detected with anti-phosphoserine in the immunoprecipitated Kv1.1 from mouse cortical membrane extracts (**Supplementary Fig. 7**). These data demonstrated that the level of tyrosine-phosphorylation of the Kv1.1 channel protein was regulated by NRG1 signaling.

To further confirm a modulation by NRG1-ErbB4 signaling of the Kv1.1 channel in parvalbumin interneurons, we investigated the tyrosine phosphorylation of Kv1.1 in the *Pvalb-cre;Erbb4*$^{-/-}$ mice. The phosphorylation of Kv1.1 was lower in the *Pvalb-cre;Erbb4*$^{-/-}$ mice than in control *Erbb4*$^{loxP/loxP}$ mice (67.7 ± 5.6% of control; $P < 0.001$, **Fig. 5h**). This result suggest that the Kv1.1 channel is regulated by NRG1-ErbB4 signaling in parvalbumin interneurons.

Increased seizure susceptibility in *Pvalb-cre;Erbb4*$^{-/-}$ mice

To assess the pathophysiological consequences of NRG1-ErbB4 dysfunction in FS-PV interneurons, we measured seizure susceptibility in *Pvalb-cre;Erbb4*$^{-/-}$ mice. We gave *Erbb4*$^{loxp/loxp}$ and *Pvalb-cre;Erbb4*$^{-/-}$ mice the common convulsant agent pentylenetetrazole (PTZ), which is considered to be a GABA receptor antagonist. The *Pvalb-cre;Erbb4*$^{-/-}$ mice developed higher seizure stages (2.7 ± 0.4 to 4.4 ± 0.38; $P < 0.05$) and a greater percentage of generalized seizures (22.2% to 75%; $P < 0.05$) than the *Erbb4*$^{loxp/loxp}$ mice. We also injected pilocarpine and quantified the percentage of mice that developed status epilepticus. More than half of the *Pvalb-cre;Erbb4*$^{-/-}$ mice developed status epilepticus, whereas the *Erbb4*$^{Loxp/Loxp}$ mice were less likely to suffer from status epilepticus (10% to 56%; $P < 0.05$). Thus, with both chemoconvulsants, loss of ErbB4 in parvalbumin interneurons increased seizure susceptibility.

Our findings predict that pharmacological stimulation of the NRG1-ErbB4 axis should contribute to anticonvulsant action. To test this, we increased extracellular NRG1 in *Erbb4*$^{Loxp/Loxp}$ mice by intracerebroventricular delivery of recombinant NRG1 20 min before PTZ or pilocarpine application. All mice developed generalized seizures within 30 min of administrating PTZ (60 mg per kilogram body weight); however, the mice given NRG1 showed lower seizure stages (5.6 ± 0.2 to 5.0 ± 0.2; $P < 0.05$) and less frequent generalized seizures than mice given vehicle (3.0 ± 0.3 to 1.5 ± 0.3; $P < 0.01$). In the pilocarpine group, NRG1 treatment greatly reduced the percentage of mice that developed status epilepticus (89% to 40%; $P < 0.05$) and delayed the onset of seizures (33.5 ± 2.1 min to 54.5 ± 7.7 min; $P < 0.05$).

Decreased ErbB4 expression in human epileptogenic tissue

To further demonstrate the link between ErbB4 and epilepsy, we used immunoblotting to assess the expression of ErbB4 in cell membranes from the epileptogenic foci in subjects with temporal lobe epilepsy (TLE) and in samples from control individuals. The level of ErbB4 protein in TLE samples was only about 60% of that in the control group (**Fig. 6a**,**b** and **Supplementary Fig. 6**); by contrast, the expression of ErbB2 was not different from that in the control group in subjects with TLE (**Fig. 6a**,**b**).

Considering that the individuals with TLE had undergone more than 2 years of medical therapy, we wondered whether anticonvulsant medication altered the expression of ErbB4. We previously investigated the

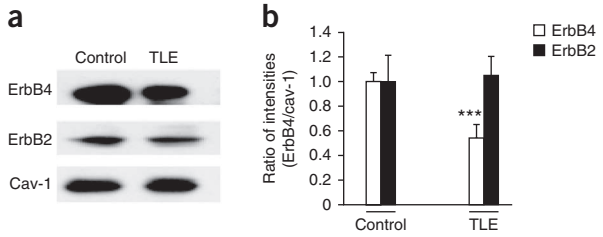

Figure 6 Decreased ErbB4 expression in human epileptogenic tissue. (**a**) Immunoblotting with ErbB4 and ErbB2 in the membrane fraction of cortex from control individuals or individuals with TLE. Western blotting with caveolin-1 (cav-1) antibody shows equal protein loading. (**b**) Quantification of ErbB4 (180 kDa) and ErbB2 (180 kDa) proteins in control and TLE groups. $n = 4$, $^{***}P < 0.001$. Error bars represent s.e.m. Full-length blots are presented in **Supplementary Figure 6**.

effects of chronic treatment with valproic acid (260 mg kg^{-1}) or sodium phenytoin (10 mg kg^{-1}) on the expression of ErbB4 in mice[35]. Both are clinically used anticonvulsant drugs[36,37]. ErbB4 expression in the mice treated with valproic acid or sodium phenytoin did not significantly differ from those treated with vehicle (**Supplementary Fig. 8**).

DISCUSSION

The main findings of this study are as follows. First, exogenous NRG1 increased the excitability of FS-PV interneurons, but this was inhibited by the neutralizing peptide ecto-ErbB4. Second, blockade or ablation of ErbB4 in parvalbumin interneurons blocked the firing potentiation by NRG1, suggesting that this effect of NRG1 is dependent on its receptor ErbB4. Third, the voltage threshold for action potential generation shifted toward more hyperpolarized levels and the near-threshold responsiveness increased after NRG1 treatment. Notably, we found that the shift of voltage threshold was mediated by inhibition of Kv1.1 voltage-gated potassium channels. Fourth, *Pvalb-cre;Erbb4*$^{-/-}$ mice were much more susceptible to PTZ- and pilocarpine-induced models of epilepsy, and seizures were ameliorated by NRG1. Finally, we showed that the expression of ErbB4 protein in the epileptogenic foci from individuals with TLE was reduced. In sum, our study identified Kv1.1 as a downstream target of NRG1-ErbB4 signaling in the regulation of interneuronal excitability. These findings suggest that the level of NRG1-ErbB4-Kv1.1 signaling is a risk factor for epilepsy.

It has been shown that NRG1 regulates pyramidal neuron activity and LTP by means of GABAergic transmission[14,15]. All these studies suggest that GABAergic interneurons are a major cellular target of NRG1-ErbB4 signaling. In the present study, we provide evidence that NRG1-ErbB4 directly regulates FS-PV interneuronal intrinsic excitability and, furthermore, that this effect does not occur through the regulation of synaptic inputs, because the effects of NRG1 were not blocked by the application of picrotoxin, DL-AP5 and DNQX. Parvalbumin interneurons have a fast-spiking firing pattern[2,38] and are the dominant inhibitory system in neocortex. They preferentially project their axons onto the perisomatic region of target neurons, regulating the output of pyramidal neurons[2]. The NRG1 regulation of pyramidal neuron activity and LTP by GABAergic release[14,15] may therefore occur downstream of regulating the excitability of interneurons by NRG1. In our study, this was confirmed because in the presence of picrotoxin NRG1 was no longer able to suppress pyramidal neuronal activity, suggesting that NRG1-ErbB4 does not directly regulate the activity of pyramidal neurons.

Electron microscopy and immunofluorescence studies show that Kv1.1-containing potassium channels are specifically localized to the axon initial segment of interneurons in cortex[32,39]. These channels powerfully influence the excitability of fast-spiking cells through regulation of voltage threshold and near-threshold responsiveness[18,40]. Our results showed that NRG1 influenced the excitability of FS-PV cells by regulating the near-threshold responsiveness and voltage threshold of the action potential, and this effect was blocked by the Kv1.1 subunit-specific blocker DTx-K, suggesting that the Kv1.1 potassium channel is a molecular target of NRG1-ErbB4 signaling. This conclusion is further supported the powerful inhibitory effect of endogenous NRG1 on Kv1.1 channel current. It has been shown that tyrosine phosphorylation suppresses the whole-cell outward current of this channel[41–43]. Indeed, we found that NRG1 increased the tyrosine phosphorylation of Kv1.1 in membrane. These results suggest for the first time the possible involvement of tyrosine phosphorylation of Kv1.1 protein by the tyrosine kinase of the ErbB4 receptor. Future studies are necessary to investigate the underlying molecular mechanisms.

Consistent with the powerful inhibition of FS-PV interneuronal excitability by NRG1-ErbB4 signaling, deletion of ErbB4 in parvalbumin interneurons led to a high seizure sensitivity in mice. Moreover, expression of ErbB4, but not ErbB2, was decreased in human epileptogenic tissue. Our findings suggest that downregulation of NRG1-ErbB4 signaling contributes to human epilepsy through decreasing the excitability of FS-PV interneurons. It has been reported that deletion of some genes regulating excitability in fast-spiking interneurons, such as *Kcnc2* (encoding Kv3.2)[3] and *Scn1a* (ref. 4), leads to epilepsy in mice. Those studies all support the idea that dysfunctional FS-PV interneuronal inhibition is involved in the etiopathogenesis of seizures[3,4]. There is a bidirectional relation between schizophrenia and epilepsy, and the two diseases may share genes and biological phenotypes[44]. Considering that *NRG1* and *ERBB4* are known to be schizophrenia susceptibility genes, it would be worthwhile to determine whether they are also epilepsy susceptibility genes. In addition, our result that NRG1 reduces seizures suggests that ErbB4 may be a new target for anticonvulsant effects in the epilepsies.

Point mutations in the Kv1.1 gene *KCNA1* and mutations in Kv1.1-associated proteins have been described in human epilepsy syndromes[45–48]. Ablation of Kv1.1 in the hippocampus produces profound epilepsy in mice[49]. Our results imply that suppressing the inhibition of FS-PV interneuronal excitability by Kv1.1 may contribute to the increased susceptibility to seizures in mice lacking ErbB4 proteins. This therefore raises the possibility that the observed phenotype in Kv1.1 knockout mice might be mainly due to pyramidal cell dysfunction. The exact cellular basis of this pathology remains unclear. Future work is required to investigate Kv1.1 effects in interneurons and pyramidal neurons, by using respectively *Pvalb-Kcna1* and *Camk2a-Kcna1* conditional knockout mice instead of *Kcna1*$^{-/-}$ (Kv1.1 null) knockout mice.

Cre expression in *Pvalb-cre;Erbb4*$^{-/-}$ mice occurs on postnatal day 13. This late-onset deletion may not cause developmental deficits that require early gene deletion. For example, mIPSCs are unchanged in *Pvalb-cre;Erbb4*$^{-/-}$ hippocampus[14]. When ErbB4 is ablated by recombination from *Dlx5/6-cre*, which begins to be expressed at embryonic day 13.5, mice have a reduced frequency of mIPSCs in pyramidal neurons[9]. Therefore, the NRG1-ErbB4 regulation of FS-PV interneuronal excitability and increased sensitivity to epilepsy in *Pvalb-cre;Erb4*$^{-/-}$ mice may be not due to developmental deficits in interneurons.

Overall, our work identifies Kv1.1 channel as a new molecular target of NRG1-ErbB4 signaling in the regulation of FS-PV interneuronal excitability and reveals that NRG1-ErbB4-Kv1.1 signaling may function in the pathology of epilepsy. Our findings also suggest that ErbB4 might be targeted to attain anticonvulsant effects in the epilepsies.

METHODS

Methods and any associated references are available in the online version of the paper at http://www.nature.com/natureneuroscience/.

Note: Supplementary information is available on the Nature Neuroscience website.

ACKNOWLEDGMENTS

We thank L. Mei (Georgia Health Sciences University) for advice. We are grateful to T.M. Gao (Southern Medical University), Z.J. Huang (Cold Spring Harbor), X.H. Zhang (Institute of Neuroscience, Chinese Academy of Sciences) and L. Bao (Institute of Biochemistry and Cell Biology, Chinese Academy of Sciences) for providing reagents and/or mice. We express our gratitude to the subjects and their families for their participation. We also thank T.M. Gao and I.C. Bruce for critical reading of this manuscript, and Q.L. Miao for technical assistance. This work was supported by grants from the National Natural Science Foundation of China (30970916, 31070926 and 30725047), the Major Research Program from the state Ministry of Science and Technology of China (2010CB912004, 2010CB912002), the Zhejiang Provincial Natural Science Foundation of China (Z2090127), the Foundation for the Author of National Excellent Doctoral Dissertation of China (200937), the Science Foundation of Chinese Universities (JD09023), the Zhejiang Provincial Qianjiang Talent Plan (2010R10057), the Fundamental Research Funds for the Central Universities (2011XZZX002) and Zhejiang Province Key Technology Innovation Team (2010R50049).

AUTHOR CONTRIBUTIONS

K.-X.L. conducted the electrophysiological studies, analyzed data and wrote the manuscript; Y.-M.L. conducted the western blot analyses and wrote the manuscript; Z.-H.X. performed the studies on the mouse model of epilepsy and analyzed data; J.Z. performed the immunostaining experiments; J.-M. Zhu and J.-M. Zhang performed surgery, provided the human tissues and analyzed data; S.-X.C. conducted part of the electrophysiological recording and gene identification; X.-J.C. purified the compounds; Z.C., S.D. and J.-H.L. contributed experimental suggestions; X.-M.L. supervised all phases of the project and wrote the manuscript.

COMPETING FINANCIAL INTERESTS

The authors declare no competing financial interests.

Published online at http://www.nature.com/natureneuroscience/.
Reprints and permissions information is available online at http://www.nature.com/reprints/index.html.

1. Perucca, E., Alexandre, V. Jr. & Tomson, T. Old versus new antiepileptic drugs: the SANAD study. *Lancet* **370**, 313; author reply 315–316 (2007).
2. Kawaguchi, Y. & Kubota, Y. GABAergic cell subtypes and their synaptic connections in rat frontal cortex. *Cereb. Cortex* **7**, 476–486 (1997).
3. Lau, D. *et al.* Impaired fast-spiking, suppressed cortical inhibition, and increased susceptibility to seizures in mice lacking Kv3.2 K+ channel proteins. *J. Neurosci.* **20**, 9071–9085 (2000).
4. Ogiwara, I. *et al.* Na(v)1.1 localizes to axons of parvalbumin-positive inhibitory interneurons: a circuit basis for epileptic seizures in mice carrying an Scn1a gene mutation. *J. Neurosci.* **27**, 5903–5914 (2007).
5. Buonanno, A. The neuregulin signaling pathway and schizophrenia: from genes to synapses and neural circuits. *Brain Res. Bull.* **83**, 122–131 (2010).
6. Mei, L. & Xiong, W.C. Neuregulin 1 in neural development, synaptic plasticity and schizophrenia. *Nat. Rev. Neurosci.* **9**, 437–452 (2008).
7. Corfas, G., Roy, K. & Buxbaum, J.D. Neuregulin 1-erbB signaling and the molecular/cellular basis of schizophrenia. *Nat. Neurosci.* **7**, 575–580 (2004).
8. Lai, C. & Lemke, G. An extended family of protein-tyrosine kinase genes differentially expressed in the vertebrate nervous system. *Neuron* **6**, 691–704 (1991).
9. Fazzari, P. *et al.* Control of cortical GABA circuitry development by Nrg1 and ErbB4 signalling. *Nature* **464**, 1376–1380 (2010).
10. Huang, Y.Z. *et al.* Regulation of neuregulin signaling by PSD-95 interacting with ErbB4 at CNS synapses. *Neuron* **26**, 443–455 (2000).
11. Yau, H.J., Wang, H.F., Lai, C. & Liu, F.C. Neural development of the neuregulin receptor ErbB4 in the cerebral cortex and the hippocampus: preferential expression by interneurons tangentially migrating from the ganglionic eminences. *Cereb. Cortex* **13**, 252–264 (2003).
12. Vullhorst, D. *et al.* Selective expression of ErbB4 in interneurons, but not pyramidal cells, of the rodent hippocampus. *J. Neurosci.* **29**, 12255–12264 (2009).
13. Woo, R.S. *et al.* Neuregulin-1 enhances depolarization-induced GABA release. *Neuron* **54**, 599–610 (2007).
14. Wen, L. *et al.* Neuregulin 1 regulates pyramidal neuron activity via ErbB4 in parvalbumin-positive interneurons. *Proc. Natl. Acad. Sci. USA* **107**, 1211–1216 (2010).
15. Chen, Y.J. *et al.* ErbB4 in parvalbumin-positive interneurons is critical for neuregulin 1 regulation of long-term potentiation. *Proc. Natl. Acad. Sci. USA* **107**, 21818–21823 (2010).
16. Kwon, O.B., Longart, M., Vullhorst, D., Hoffman, D.A. & Buonanno, A. Neuregulin-1 reverses long-term potentiation at CA1 hippocampal synapses. *J. Neurosci.* **25**, 9378–9383 (2005).
17. Pitcher, G.M. *et al.* Schizophrenia susceptibility pathway neuregulin 1-ErbB4 suppresses Src upregulation of NMDA receptors. *Nat. Med.* **17**, 470–478 (2011).
18. Goldberg, E.M. *et al.* K+ channels at the axon initial segment dampen near-threshold excitability of neocortical fast-spiking GABAergic interneurons. *Neuron* **58**, 387–400 (2008).
19. Chattopadhyaya, B. *et al.* Experience and activity-dependent maturation of perisomatic GABAergic innervation in primary visual cortex during a postnatal critical period. *J. Neurosci.* **24**, 9598–9611 (2004).
20. Di Cristo, G. *et al.* Subcellular domain-restricted GABAergic innervation in primary visual cortex in the absence of sensory and thalamic inputs. *Nat. Neurosci.* **7**, 1184–1186 (2004).
21. Law, A.J., Shannon Weickert, C., Hyde, T.M., Kleinman, J.E. & Harrison, P.J. Neuregulin-1 (NRG-1) mRNA and protein in the adult human brain. *Neuroscience* **127**, 125–136 (2004).
22. Ting, A.K. *et al.* Neuregulin 1 promotes excitatory synapse development and function in GABAergic interneurons. *J. Neurosci.* **31**, 15–25 (2011).
23. Bjarnadottir, M. *et al.* Neuregulin1 (NRG1) signaling through Fyn modulates NMDA receptor phosphorylation: differential synaptic function in NRG1+/– knock-outs compared with wild-type mice. *J. Neurosci.* **27**, 4519–4529 (2007).
24. Gu, Z., Jiang, Q., Fu, A.K., Ip, N.Y. & Yan, Z. Regulation of NMDA receptors by neuregulin signaling in prefrontal cortex. *J. Neurosci.* **25**, 4974–4984 (2005).
25. Li, B., Woo, R.S., Mei, L. & Malinow, R. The neuregulin-1 receptor erbB4 controls glutamatergic synapse maturation and plasticity. *Neuron* **54**, 583–597 (2007).
26. Fukazawa, R. *et al.* Neuregulin-1 protects ventricular myocytes from anthracycline-induced apoptosis via erbB4-dependent activation of PI3-kinase/Akt. *J. Mol. Cell. Cardiol.* **35**, 1473–1479 (2003).
27. García-Rivello, H. *et al.* Dilated cardiomyopathy in Erb-b4-deficient ventricular muscle. *Am. J. Physiol. Heart Circ. Physiol.* **289**, H1153–H1160 (2005).
28. Arber, S., Ladle, D.R., Lin, J.H., Frank, E. & Jessell, T.M. ETS gene Er81 controls the formation of functional connections between group Ia sensory afferents and motor neurons. *Cell* **101**, 485–498 (2000).
29. Hippenmeyer, S. *et al.* A developmental switch in the response of DRG neurons to ETS transcription factor signaling. *PLoS Biol.* **3**, e159 (2005).
30. Fisahn, A., Neddens, J., Yan, L. & Buonanno, A. Neuregulin-1 modulates hippocampal gamma oscillations: implications for schizophrenia. *Cereb. Cortex* **19**, 612–618 (2009).
31. Neddens, J. & Buonanno, A. Selective populations of hippocampal interneurons express ErbB4 and their number and distribution is altered in ErbB4 knockout mice. *Hippocampus* **20**, 724–744 (2010).
32. Coetzee, W.A. *et al.* Molecular diversity of K+ channels. *Ann. NY Acad. Sci.* **868**, 233–285 (1999).
33. Guan, D. *et al.* Expression and biophysical properties of Kv1 channels in supragranular neocortical pyramidal neurones. *J. Physiol. (Lond.)* **571**, 371–389 (2006).
34. Robertson, B., Owen, D., Stow, J., Butler, C. & Newland, C. Novel effects of dendrotoxin homologues on subtypes of mammalian Kv1 potassium channels expressed in *Xenopus* oocytes. *FEBS Lett.* **383**, 26–30 (1996).
35. Ziyatdinova, S. *et al.* Spontaneous epileptiform discharges in a mouse model of Alzheimer's disease are suppressed by antiepileptic drugs that block sodium channels. *Epilepsy Res.* **94**, 75–85 (2011).
36. Dreyfus, J. *A Remarkable Medicine Has Been Overlooked: Including an Autobiography and the Clinical Section of the Broad Range of Use of Phenytoin* (Continuum International Publishing Group, 1998).
37. Perucca, E. Pharmacological and therapeutic properties of valproate: a summary after 35 years of clinical experience. *CNS Drugs* **16**, 695–714 (2002).
38. Gibson, J.R., Beierlein, M. & Connors, B.W. Two networks of electrically coupled inhibitory neurons in neocortex. *Nature* **402**, 75–79 (1999).
39. Wang, H., Kunkel, D.D., Schwartzkroin, P.A. & Tempel, B.L. Localization of Kv1.1 and Kv1.2, two K channel proteins, to synaptic terminals, somata, and dendrites in the mouse brain. *J. Neurosci.* **14**, 4588–4599 (1994).
40. Tanouye, M.A., Ferrus, A. & Fujita, S.C. Abnormal action potentials associated with the Shaker complex locus of *Drosophila*. *Proc. Natl. Acad. Sci. USA* **78**, 6548–6552 (1981).
41. Holmes, T.C., Fadool, D.A., Ren, R. & Levitan, I.B. Association of Src tyrosine kinase with a human potassium channel mediated by SH3 domain. *Science* **274**, 2089–2091 (1996).
42. Cook, K.K. & Fadool, D.A. Two adaptor proteins differentially modulate the phosphorylation and biophysics of Kv1.3 ion channel by SRC kinase. *J. Biol. Chem.* **277**, 13268–13280 (2002).
43. Tucker, K. & Fadool, D.A. Neurotrophin modulation of voltage-gated potassium channels in rat through TrkB receptors is time and sensory experience dependent. *J. Physiol. (Lond.)* **542**, 413–429 (2002).
44. Cascella, N.G., Schretlen, D.J. & Sawa, A. Schizophrenia and epilepsy: is there a shared susceptibility? *Neurosci. Res.* **63**, 227–235 (2009).
45. Zuberi, S.M. *et al.* A novel mutation in the human voltage-gated potassium channel gene (Kv1.1) associates with episodic ataxia type 1 and sometimes with partial epilepsy. *Brain* **122**, 817–825 (1999).
46. Liguori, R., Avoni, P., Baruzzi, A., Di Stasi, V. & Montagna, P. Familial continuous motor unit activity and epilepsy. *Muscle Nerve* **24**, 630–633 (2001).
47. Schulte, U. *et al.* The epilepsy-linked Lgi1 protein assembles into presynaptic Kv1 channels and inhibits inactivation by Kvbeta1. *Neuron* **49**, 697–706 (2006).
48. Strauss, K.A. *et al.* Recessive symptomatic focal epilepsy and mutant contactin-associated protein-like 2. *N. Engl. J. Med.* **354**, 1370–1377 (2006).
49. Smart, S.L. *et al.* Deletion of the K(V)1.1 potassium channel causes epilepsy in mice. *Neuron* **20**, 809–819 (1998).

ONLINE METHODS

Reagents and mice. The NRG1 used is a recombinant polypeptide containing the entire EGF domain of β-type Neuregulin 1 (Prospec). The coding sequence for the ecto-domain of ErbB4 (amino acids 1–659, ecto-ErbB4) was subcloned into pC4DNA/Fc to generate pErbB4ex/Fc. HEK-293 cells stably expressing ecto-ErbB4 were generated and cultured in low–immunoglobulin G medium for collection of conditioned medium. ErbB4ex/Fc was purified by a HiTrap column (Amersham). DL-2-Amino-5-phosphonovaleric acid (DL-AP5), DNQX, TTX and picrotoxin were purchased from Tocris Bioscience and DTx-K from Alomone Labs. PTZ was from Research Biochemicals, valproic acid from Sanofi Aventis and sodium phenytoin from Tianjing Lisheng. Other chemicals were from Sigma-Aldrich. When necessary, chemicals were dissolved in dimethylsulfoxide (DMSO, Sigma); the final concentration of DMSO was <0.01% when applied to brain slices.

Primary antibodies used were rat monoclonal anti-Kv1.1 (NeuroMab), mouse monoclonal anti-phosphotyrosine (P-Tyr-102, Cell Signaling Technology), mouse monoclonal anti- phosphoserine (p-Ser (1C8), Santa Cruz Biotechnology, Inc.), mouse monoclonal anti-parvalbumin (PV235, Swant), rabbit anti-ErbB4 (Santa Cruz Biotechnology), rabbit anti-ErbB2 (Santa Cruz Biotechnology), rabbit anti-caveolin-1 (Cell Signaling Technology) and mouse monoclonal anti–β-actin (Sigma). DAPI was used to stain nuclei.

Transgenic mice lines B13 and G42, expressing enhanced green fluorescent protein (EGFP) in parvalbumin interneurons, have been well characterized[2,19,20] for effectively targeting fast-spiking cells. ErbB4 conditional knockout mice were generated by a *loxP*-Cre strategy. *Pvalb-cre* mice were crossed with mice carrying a *loxP*-flanked *Erbb4* gene to generate *Pvalb-cre;Erbb4*$^{-/-}$ mice, with *Erbb4*$^{loxP/loxP}$ mice as a control. To assist electrophysiological recording of parvalbumin interneurons, the conditional mutant mice were further crossed with *G42;Erbb4*$^{loxP/loxP}$ mice. All mice were housed under a 12-h light/dark cycle and had access to food and water *ad libitum*. The use and care of the mice complied with the guidelines of the Animal Advisory Committee at Zhejiang University and the US National Institutes of Health Guidelines for the Care and Use of Laboratory Animals. In total, about 287 mice were used in this work. For behavioral experiments, only male mice were used.

Slice preparation. We made coronal slices of the cortex or hippocampus from mice about 4 weeks old. Slices (300 μm) were prepared with a Vibroslice (Leica VT 1000S) in ice-cold artificial cerebrospinal fluid (ACSF), which consisted of 125 mM NaCl, 3 mM KCl, 1.25 mM NaH_2PO_4, 2 mM $MgSO_4$, 2 mM $CaCl_2$, 25 mM $NaHCO_3$ and 10 mM glucose. After recovery for ~60 min, incubation in ACSF at 33 °C was followed by ~60 min at 22 °C, when slices were transferred to the recording chamber and superfused (3 ml min^{-1}) with ACSF at 32–33 °C. All solutions were saturated with 95% O_2, 5% CO_2.

Electrophysiology. Neurons were visualized with an infrared-sensitive CCD camera with a ×40 water-immersion lens (Nikon, ECLIPSE FN1) and recorded using whole-cell techniques (MultiClamp 700B Amplifier, Digidata 1440A analog-to-digital converter) and pClamp 10.2 software (Axon Instruments/Molecular Devices). For action potential recording, glass pipettes (3–4 MΩ) were filled with a solution containing 130 mM potassium gluconate, 20 mM KCl, 10 mM HEPES buffer, 4 mM Mg-ATP, 0.3 mM Na-GTP, 10 mM disodium phosphocreatine and 0.2 mM EGTA, pH 7.2 with KOH, 288 mOsm. ISI, calculated for averaged intervals between sequential action potentials in a train elicited in response to a 500-ms suprathreshold current of 400 to 800 pA, was used to quantify the excitability of FS-PV interneurons. The shape parameters were measured from action potentials evoked by 500-ms current injection. Voltage threshold was defined as $dV/dt = 10$ mV ms^{-1}. The slope of initiation was measured as the slope from the trough voltage of action potential repolarization to the subsequent voltage before action potential initiation. Spike amplitude was measured as the voltage difference between the peak and the threshold of the action potential. Fast afterhyperpolarization was measured as the difference between the spike threshold and minimum voltage after the action potential peak. Spike width was measured at half the spike amplitude. Firing adaptation (ISI_1/ISI_n) was calculated by dividing the averaged last five ISIs evoked by suprathreshold current by the first interval of the train. Threshold current for spike generation (I_{TH}) was the minimum depolarizing current needed to elicit at least one action potential. Membrane time constant (τ) was measured using a single exponential fit of the voltage deflection produced by small hyperpolarizing current injection from resting membrane potential. All analysis was performed using customized routines in Matlab.

To measure the potassium channel currents in voltage clamp, the patch pipette (3–4 MΩ) was filled with the same solution as for current-clamp recording. We applied a series of voltage pulses from −80 mV to −20 mV for 3 s and generated an outward current. Currents were evoked by voltage steps up to −20 mV. This enabled us to investigate low-threshold currents without introducing series resistance errors associated with large currents. For GABAergic postsynaptic current recordings, a symmetric chloride internal solution (in mM) was used for recording IPSCs: 120 mM KCl, 20 mM potassium gluconate, 10 mM HEPES, 2 mM $MgCl_2$, 4 mM Mg-ATP, 0.3 mM Na-GTP 10 mM disodium phosphocreatine and 0.5 mM EGTA, pH 7.2 with KOH, 288 mOsm. To isolate spontaneous IPSCs, the ACSF contained 50 μM DL-AP5 and 20 μM DNQX. mIPSCs were recorded in the presence of 50 μM DL-AP5, 20 μM DNQX and 1 μM TTX. The holding potential for both action potential and IPSCs recordings was −70 mV. During recording, access resistance was compensated by up to 70%. Neurons with series resistance below 20 MΩ and changing <20% throughout the recording were used for analysis. Bridge balance and whole-cell compensation were carefully adjusted. Recordings were Bessel-filtered at 10 kHz and sampled at 100 kHz for action potentials and filtered at 3 kHz and sampled at 10 kHz for IPSCs and potassium current recordings.

Immunocytochemistry. Immunofluorescence staining was carried out as described previously[14]. Briefly, mice were perfused transcardially with 4% paraformaldehyde (4 g per 100 ml) and 4% sucrose (4 g per 100 ml) in PBS, pH 7.4. Brain tissues were then postfixed at 4 °C for 24 h, and coronal slices (40 μm) were prepared using a Vibroslice (VT 1000S). Brain sections were treated with 3% (vol/vol) normal goat serum in PBS containing 0.5% Triton X-100 for 1 h. Then the brain sections were incubated with ErbB4 antibody 0618 (1:400) and mouse monoclonal anti-parvalbumin (1:1,000) at 4 °C for 36–48 h. Immunoreactivity was imaged with Alexa 488– and Alexa 594–conjugated goat anti–mouse IgG (1:400).

Immunoprecipitation and immunoblotting. Brain slices were incubated with NRG1 (10 nM) for 5, 10 or 20 min, and membrane fractionation from brain slices was performed as described previously[50]. Immunoprecipitation of Kv1.1 was carried out using membrane extracts of mouse brain. Briefly, extracts containing 60 μg protein were incubated overnight at 4 °C with 10 μl of monoclonal antibody to Kv1.1, which was captured by adding Protein A–Sepharose CL-4B beads (Upstate Biotechnology) suspension (50%, vol/vol). Immunoprecipitated complexes were collected by centrifugation, then washed three times with buffer containing 50 mM Tris-HCl, pH 7.5, 0.5 mM NaCl, 4 mM EDTA, 4 mM EGTA, 1 mM Na_3VO_4, 50 mM NaF, 1 mM dithiothreitol, 1 mM PMSF, 2 μg ml^{-1} pepstatin A, 1 μg ml^{-1} leupeptin and 100 nmol l^{-1} calyculin A. After the final wash, we aspirated the supernatant and resuspended the pellet in electrophoresis sample buffer. Bound proteins were loaded on 10% acrylamide SDS-PAGE gels. Membranes with proteins were immunoblotted using antibodies to phosphotyrosine (monoclonal antibody, 1:1,000), phosphoserine (monoclonal antibody, 1:1,000), caveolin-1 (polyclonal antibody, 1:1,000), ErbB4 (polyclonal antibody, 1:500), ErbB2 (polyclonal antibody, 1:500) and β-actin (monoclonal antibody, 1:2,000). Signals were detected with enhanced chemiluminescence and developed on X-ray film. For densitometric quantification, immunoblots were digitized on a flatbed scanner and digital images were measured using the US National Institutes of Health Image program.

Behavioral assays. For seizure induction with PTZ or pilocarpine, to assess the effects of ERB4 on seizure severity, PTZ was dissolved in PBS and injected intraperitoneally at the indicated dose. After injection, the mouse was placed in a transparent Plexiglas cage and observed for up to 30 min. All the experiments were performed in the laboratory between 12:00 and 14:00. The seizure behavior was observed for 30 min using the following scale: (0) no response; (1) ear and facial twitching; (2) myoclonic body jerks; (3) clonic forelimb convulsions; (4) generalized clonic convulsions and turning onto the side; (5) generalized clonic-tonic convulsions and loss of postural control; (6) several episodes of stage 5 seizures or death within 30 min. We also scored the incidence of generalized seizures, which were identified by stage 4 and 5 seizures. We chose different PTZ doses to test specific hypotheses and decrease the overall number of mice

doi:10.1038/nn.3006

required. For example, to test the hypothesis that the *Pvalb-cre;Erbb4*$^{-/-}$ mice have more severe seizures than controls, we used a PTZ dose (40 mg kg^{-1}) that evokes generalized seizures in a small percentage of the control mice. And to efficiently test the anticonvulsant effects of NRG1, we used a PTZ dose (60 mg kg^{-1}) that evoked a severe seizure score in the ACSF control group. To score the effects of ErbB4 on seizure severity in response to pilocarpine, we investigated the incidence of status epilepticus. As with PTZ, pilocarpine was given at 200 mg kg^{-1} for comparing the percentage of mice that developed status epilepticus in *Erbb4*$^{loxP/loxP}$ and *Pvalb-cre;Erbb4*$^{-/-}$ mice and at 250 mg kg^{-1} for testing the effect of NRG1 treatment. A trained observer, who was unaware of genotype, scored seizure severity.

For NRG1 administration, mice were mounted under isoflurane anesthesia (2%) in a stereotaxic apparatus (512600, Stoelting) and NRG1 (6 mmol in 3 µl) was injected into the right lateral ventricle (anteroposterior, −0.5 mm from bregma; lateral, −1 mm; ventral, −2.2 mm) over the course of 5 min. After 15 min recovery, mice were given PTZ or pilocarpine intraperitoneally once and behavior was scored as above.

Human material. We used cortical tissue from the temporal lobes of five people with intractable epilepsy or brain trauma conforming to the following criteria: (i) typical epilepsy symptoms and electroencephalographic features, seizures persisting despite more than 2 years of medical therapy with three or more kinds of antiepileptic first-line drugs with effective blood drug concentrations; (ii) seizure syndromes fitting the 1981 International Anti-epilepsy Federation classification; (iii) no progressive foci found after computed tomography and magnetic resonance imaging examination; (iv) no other nervous system disease other than epilepsy and no potential inducing causes; and (v) localization-related epileptiform discharges in preoperative evaluation and operative indications. Control group criteria: (i) no history of central nervous system disease; and (ii) no structural and functional injury that can induce epilepsy other than trauma. There was no statistical difference in age between the groups. Written informed consent was obtained from both epilepsy and control subjects and signed by subjects and legal guardians. The research was approved by the Medical Ethical Committee of Zhejiang University School of Medicine (No. 1-009).

Brain stereotactic identification was carried out by comprehensive analysis of clinical manifestations, sphenoidal electrode recording, video electroencephalogram monitoring and magnetic resonance imaging. Epileptic focus location and operation was monitored by an intraoperative neocortical electrode. Abnormal waves disappeared or were markedly reduced in the immediate electrocorticography examination after resection of foci and abnormal discharge tissue near the foci. The resected brain tissues were obtained for study.

Human tissue preparation and western blot analysis. One gram of temporal cortical tissue was dissected from fresh frozen brain sections maintained at −80 °C. We isolated the membrane fraction as described above. Membranes were immunoblotted using antibodies to ErbB4, ErbB2 and caveolin-1. Signals were detected with enhanced chemiluminescence and developed on X-ray film. For densitometric quantification, immunoblots were digitized on a flatbed scanner and the images were quantified using the US National Institutes of Health Image program.

Statistical analysis. Data are presented as mean ± s.e.m. (n = number of individual samples). For comparison of means from the same group of cells, a two-tailed Student's t-test was used. For two-group comparisons, statistical differences were calculated by two-tailed Student's t-test or by Pearson's chi-squared test.

50. Ostrom, R.S. *et al.* Receptor number and caveolar co-localization determine receptor coupling efficiency to adenylyl cyclase. *J. Biol. Chem.* **276**, 42063–42069 (2001).